Towards Targeted MRI: New MRI Contrast Agents for Sialic Acid Detection

**Luca Frullano,[a, b] Jan Rohovec,[c] Silvio Aime,[d] Thomas Maschmeyer,[a, e]
M. Isabel Prata,[f] J. J. Pedroso de Lima,[f] Carlos F. G. C. Geraldes,[g] and
Joop A. Peters*[a]**

Abstract: The detection of sialic acid in living systems is of importance for the diagnosis of several types of malignancy. We have designed and synthesized two new lanthanide ion ligands (L^1 and L^2) that are capable of molecular recognition of sialic acid residues. The basic structure of these ligands consists of a DTPA-bisamide (DTPA, diethylenetriamine pentaacetic acid) whose amide moieties each bear both a boronic function for interaction with the diol groups in the side chain of sialic acid, and a functional group that is positively charged at physiologic pH values and is designed to interact with the carboxylate anion of sialic acid. The relaxometric properties of the Gd^{3+} complexes of these two ligands were evaluated. The relaxivity of the GdL^1 complex has a significant second-sphere contribution at pH values above the pK_a of its phenylboronic acid moiety. The interaction of the Gd^{3+} complexes of L^1 and L^2 with each of several saccharides was investigated by means of a competitive fluorescent assay. The results show that both complexes recognize sialic acid with good selectivity in the presence of other sugars. The adduct formed by GdL^2 with sialic acid has the higher conditional formation constant ($50.43 \pm 4.61 \, M^{-1}$ at pH 7.4). The ability of such complexes to recognize sialic acid was confirmed by the results of a study on the interaction of corresponding radiolabeled complexes ($^{153}SmL^1$ and $^{153}SmL^2$) with C6 glioma rat cells. $^{153}SmL^2$ in particular is retained on the cell surface in significant amounts.

Keywords: borates · carbohydrates · drug design · lanthanides · magnetic resonance imaging

Introduction

The excellent contrast and spatial resolution of the images obtained by magnetic resonance imaging (MRI), particularly those of soft tissues, have made this technique one of the fastest growing diagnostic methodologies. An MRI image is generated from the NMR resonance of water protons and the contrast depends essentially on three factors, 1) the water proton density, 2) the longitudinal relaxation time, T_1, and 3) the transverse relaxation time, T_2, of these protons.[1–4] Paramagnetic contrast agents (CAs) are often administered prior to the scan to improve the contrast in the image. The role of these CAs, usually Gd^{3+} complexes, is to shorten the relaxation times of the water ^1H NMR reso-

[a] Dr. L. Frullano, Prof. Dr. T. Maschmeyer, Dr. J. A. Peters
Laboratory of Applied Organic Chemistry and Catalysis
Julianalaan 136, 2628 BL Delft (The Netherlands)
Fax: (+31)15-278-4289
E-mail: j.a.peters@tnw.tudelft.nl

[b] Dr. L. Frullano
Chemistry Department
Northwestern University
Evanston, Illinois 60208-3113 (USA)

[c] Dr. J. Rohovec
Department of Chemistry
Universita Karlova
12840 Prague (Czech Republic)

[d] Prof. S. Aime
Dipartimento di Chimica I.F.M.
Università di Torino
10125 Torino (Italy)

[e] Prof. Dr. T. Maschmeyer
School of Chemistry
The University of Sydney
NSW 2006 (Australia)

[f] Dr. M. I. Prata, Prof. Dr. J. J. P. de Lima
Department of Biophysics of the Faculty of Medicine
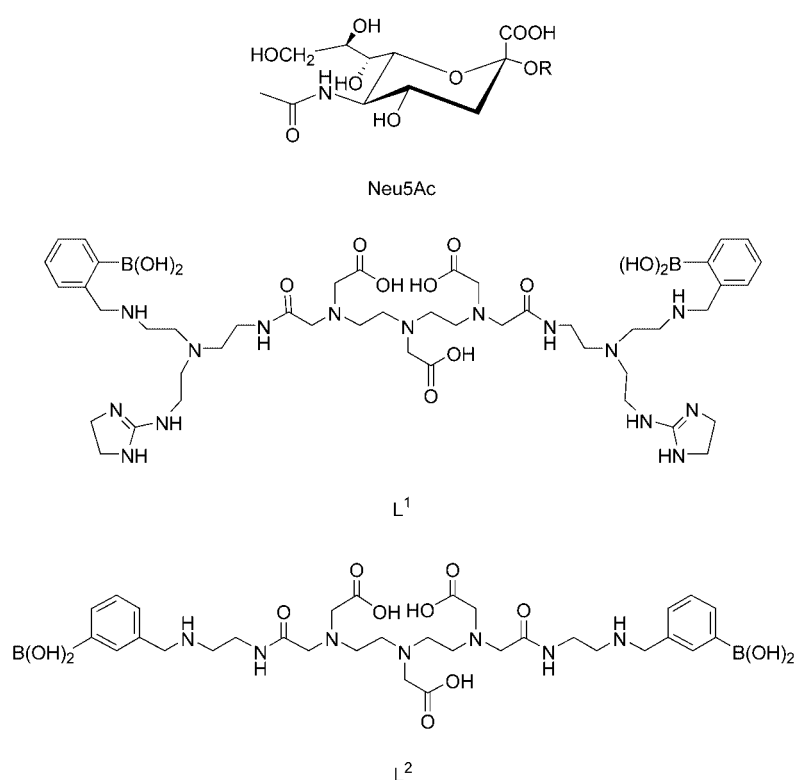University of Coimbra
3000 Coimbra (Portugal)

[g] Prof. Dr. C. F. G. C. Geraldes
Departamento de Ciências e Tecnologica e
Centro Neurociências
Universidade de Coimbra
3049 Coimbra (Portugal)

nance. CAs currently on the market suffer from several disadvantages, the most important of which are poor efficiency with regard to the shortening of T_1 and T_2, and a lack of specificity. Once administered, these agents rapidly equilibrate nonspecifically between the intravascular and the interstitial compartments. For this reason, a great deal of attention has been dedicated to the development of new and more efficient contrast agents.[5,6] The delivery of higher doses of CA to the target site through the exploitation of receptors or molecular determinants would improve visualization of abnormalities and the CA could be used to obtain not only anatomical information but also information at the molecular level. Molecular imaging would make it possible to study and understand cellular events or to monitor gene delivery and expression in gene therapy.[7–10]

Scheme 1. Molecular structures of a Neu5Ac end group in a glycoprotein or glycolipid (R) and the targeting ligands L^1 and L^2.

A major difficulty in the development of targeted CAs is the very low concentration of receptors (10^{-9}–10^{-13} mol g^{-1}) in tissues, combined with the low intrinsic sensitivity of MRI.[11] Several approaches have been applied to this problem and some progress has been made by using monoclonal antibodies (mAbs) covalently conjugated with MRI CAs. However, modification of mAbs can alter their affinity towards the target as well as their pharmacokinetic properties.[4] There is thus considerable interest in the development of alternative targeting strategies.

Receptors often consist of carbohydrates on glycoproteins or glycolipids, and in many cases sialic acids are involved. The sialic acids are a family of C_9 monosaccharides with a carboxy group at the anomeric carbon atom ($pK_a = 2.2$) that gives the molecule a negative charge at physiological pH (Scheme 1). These compounds frequently occur as the terminal residue of a glycan chain in a glycoprotein or glycolipid present on the cell surface or in an intracellular membrane (e.g. Golgi apparatus). The biological roles played by sialic acids are the result of the physicochemical properties of these molecules (size, hydrophilicity, and negative charge at physiological pH) and of their exposed positions in glycan chains. They appear to be involved in the binding and transport of positively charged ions or molecules and in the attraction and repulsion of cells and molecules. Sialic acids can also act as a protective shield for the subterminal portion of a molecule, but their most important functions concern cellular and molecular recognition.[12–16]

Sialic acid concentration has been proposed as a prognostic and diagnostic indicator for several diseases. In particu-

lar, a correlation between an altered sialylation pattern and lowered defensive activity against viral infections and tumor cells has been reported.[17] Lemieux et al. took advantage of the overexpression of sialic acid on tumor cell surfaces (up to 10^9 sialic acid residues per tumor cell as compared to only 20×10^6 for a normal human erythrocyte) to detect tumor cells.[18] By supplying *N*-levulinoylmannosamine, an unnatural substrate for the sialoside biosynthetic pathway, to Jurkat cells these authors were able to convert the substrate into *N*-levulinoyl sialic acid, a ketone-substituted sialic acid. This keto group can be used as an anchor for covalent binding of an aminoxy-substituted GdDTPA (DTPA, diethylenetriamine pentaacetic acid), which results in contrast enhancement and may make the molecule observable in an MRI image.

Herein, we report the results of studies on two Gd^{3+} complexes (GdL^1 and GdL^2) built with ligands containing DTPA and phenylboronate functions (see Scheme 1). These complexes were designed to interact reversibly with sialic acid. The advantage of this approach is that the contrast agent is in a dynamic equilibrium between its sialic-acid-bound and free states. The free complex can eventually be excreted by the normal physiological mechanism, which shifts the equilibrium away from the bound form.

Many efforts have been made to develop biomimetic sugar receptors that operate in water.[19,20] However, the only promising class of sugar receptors developed so far is that of the arylboronic acids, which are not biomimetic.[21] The ability of boric and phenylboronic acid to interact with sugars has been known for a long time.[22–24] Phenylboronic

acid is a weak acid ($pK_a = 8.67$)[25] that bonds covalently and reversibly with 1,2- or 1,3-diols to give five- or six-membered cyclic esters (see Scheme 2). The stability of the esters formed by the boronate anion (tetragonal) is orders of magnitude higher than that of the esters formed by boronic acid (trigonal).[26] The binding ability of boronic acid is therefore optimal under basic conditions (pH > 8–9) since the concentration of the boronate anion is maximal in such an environment.
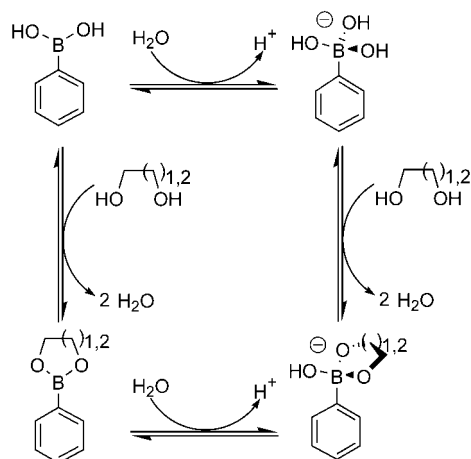
Scheme 2. The equilibria involved in a diol–boronic acid interaction.

The requirement of basic conditions for optimal interaction is a drawback for the use of these moieties in saccharide receptors. Wulff has shown that the conversion of a trigonal boronic into a tetragonal boronate function occurs at a much lower pH value when an aminomethyl group is introduced at the *ortho*-position (Scheme 3).[27,28] This effect
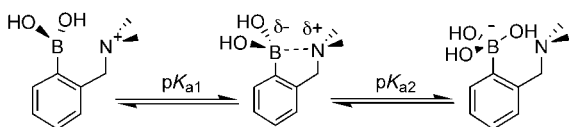
Scheme 3. The pH-dependent equilibria characteristic of an *o*-aminomethylphenylboronic acid.

can be ascribed to a B–N interaction in the phenylboronate species that results in a decrease in the pK_a value of the tertiary amino group to around 5, and an increase in that of the boronic function to about 12.[29] The presence of the tetragonal species over a broader pH range favors the interaction of this type of compound with saccharides at physiological pH levels.

We previously studied the interaction of phenylboronic acid with Neu5Ac, the most widespread form of sialic acid (Scheme 1).[30] The boronic group appeared to interact both with the glycerine moiety at C6 to form five- and six-membered cyclic esters, and with the carboxy group and the hydroxy group at C2 to form a five-membered cyclic ester. The formation constant we determined for phenylboronic

acid/Neu5Ac adduct formation is higher than those for various other monosaccharides commonly present in glycan chains on cell surfaces. Free Neu5Ac differs from sialic acid residues in glycan chains; in a glycan chain, the C2 position of the acid is involved in the glycosidic linkage, which precludes interaction with phenylboronic acid at the C1/C2 position. Consequently, it is reasonable to expect a weaker interaction between phenylboronic acid and sialic acids in glycoconjugates than between the same compound and free Neu5Ac.

To increase the specificity and stability of the interaction between the target receptor and sialic acid, we introduced another functional group to our artificial receptors in addition to phenylboronic acid. The role of this additional group is to interact with the carboxy group at the C1 position of sialic acid (Scheme 1). Guanidinium cations are very weakly acidic ($pK_a \approx 12.5$) and have the capacity to form intermolecular contacts mediated by H-bonding interactions. The guanidinium ion is present in many natural products and is often involved in molecular recognition.[31] For example, in E-selectin a guanidinium ion on an arginine residue is the binding site for the carboxylate group of sialyl Lewis X acids.[32] This example inspired us to include an aminoimidazolium group in the design of L^1 to allow binding of the carboxylate group of Neu5Ac.

Compound L^2 was designed to interact with the carboxy group at the C1 position of Neu5Ac through an aminomethyl group present in the *meta*-position of L^2 relative to the boronic function. This aminomethyl moiety is protonated under physiological conditions. The design of both ligands was completed by inclusion of a central chelating unit based on the DTPA structure, which is known to afford a stable coordination cage for lanthanide ions (see Scheme 1).[1–4] Molecular modeling studies indicate that both L^1 and L^2 can occur in conformations that allow cooperative two-site binding of sialic acid through 1) ester formation by interaction of the boronate function on the ligand with the geminal diol function at C8/C9 of Ne5Ac, and 2) an electrostatic interaction between the positively charged moiety on the ligand and the carboxylate group of Neu5Ac.

The two ligands L^1 and L^2 were synthesized and the relaxometric properties of their Gd^{3+} complexes were evaluated. Interaction of the ligands with Neu5Ac and other competing monosaccharides present in glycan chains was investigated by means of a three-component competitive fluorescence assay developed by Wang and Springsteen.[26] We exploited the excellent sensitivity of radiometric methods to investigate the interaction of the ^{153}Sm complexes of the ligands with C6 rat glioma cells. It has been shown that these cells have high membrane concentrations of sialic acid.[33]

Results and Discussion

Synthesis: The ligands prepared for this study, L^1 and L^2, are both composed of a central lanthanide-chelating unit flanked by two identical groups designed to interact with sialic acid. Ligand L^1 was synthesized from tris-(2-aminoethyl)amine (TREN). Two of the three amine functions of

this compound were protected with *tert*-butoxycarbonyl (Boc) groups by the procedure of Hamdaoui et al.,[34] which gave compound **1** (Scheme 4). Treatment of **1** with 2-methyl-thio-2-imidazoline hydroiodide in refluxing ethanol, followed by deprotection with HCl afforded **3** in excellent yield. The boronic acid function was introduced by reductive amination of **3** with 2-formylphenylboronic acid and sodium borohydride, which led to a mixture of mono- and bis-substituted derivatives of **3**. Separation of these derivatives was achieved by ion exchange chromatography on a weakly acidic cation exchanger (Amberlite CG50), with gradient elution in aqueous ammonia. Ligand **L¹** was obtained by condensation of **4** with DTPA-bisanhydride in ethanol.

The bis-Boc-protected precursor of ligand L² (**5**) was prepared by a published procedure.[35] Deprotection by treatment with TFA gave **6** almost quantitatively. Ligand L² was obtained by reductive amination of **6** with excess 3-formyl-phenylboronic acid and sodium borohydride.

¹¹B NMR shift titrations: The chemical shift of the ¹¹B resonance of ligand L¹ was recorded as a function of the pH value and was found to jump from 9.4 to −11.4 ppm, with

an inflection point at about pH 4.9. This shift change marks the transition between a trigonal and a tetragonal boron atom that results from formation of a B−N bond upon deprotonation of the amino group (see Scheme 3). By fitting the chemical shift titration curve to the appropriate equations, we determined the pK_a value of the amino group to be 4.93. This value is considerably lower than the pK_a of benzylamine ($pK_a = 9.40 \pm 0.08$, $\mu = 0.1$),[36] which demonstrates that the ammonium group is considerably stabilized by the presence of the *ortho*-boronic function. It was not possible to determine the pK_a value of the boronic function from the titration curve since no other jump in chemical shift occurred. This result indicates that the pK_a value of the boronic function is higher than 12. The observed pK_a trends agree well with those reported by Wiskur et al. for *o*-amino-methylphenylboronic acid.[29]

The situation is different for L² because the aminomethyl group is in the *meta*-position with respect to the boronic function and B–N interaction is therefore impossible. The ¹¹B NMR chemical shift change (9.4 to −16.6 ppm) with increasing pH value can, once again, be ascribed to the conversion of the boron functionality from a trigonal into a tet-
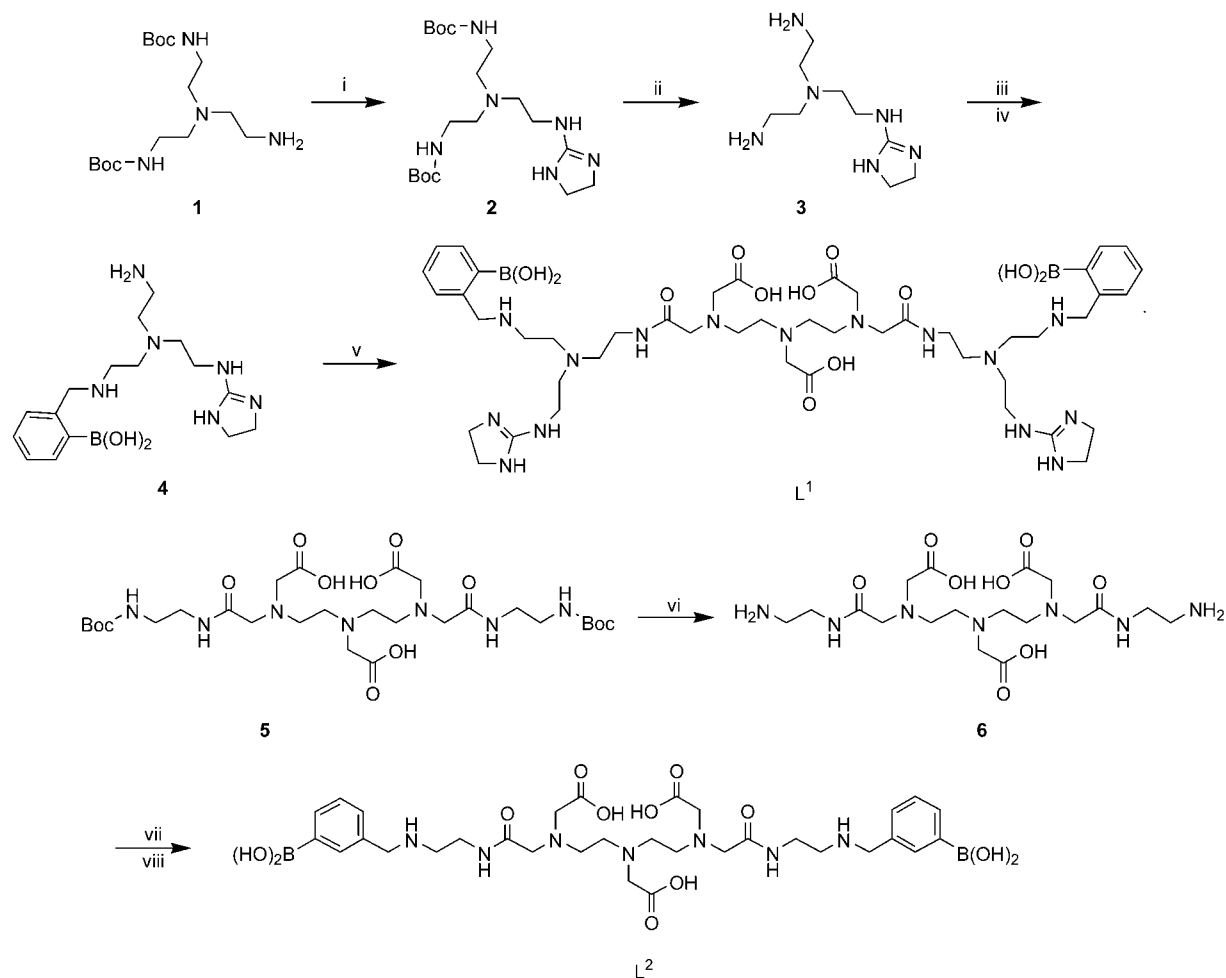
Scheme 4. Preparation of ligands L¹ and L². i) 2-methylthio-2-imidazoline hydroiodide, EtOH, 5 h, reflux; ii) HCl 37%, EtOH, 1.5 h, RT, 87%; iii) 2-for-mylphenylboronic acid, MeOH/TEA (3:1 v/v), 6 h, RT; iv) NaBH₄, 12 h, RT, 26%; v) DTPA-bisanhydride, zeolite KA, EtOH, 6 h, 95%; vi) TFA, 12 h, RT, 97%; vii) 3-formylphenylboronic acid, MeOH/TEA (2:1 v/v), 2 h, RT; viii) NaBH₄, MeOH/TEA (2:1 v/v), 12 h, RT, 90%. TEA, triethylamine; TFA, trifluoroacetic acid.

ragonal geometry (Scheme 3). In this case, this transition is the result of the reaction of the boron function with an OH⁻ ion to form a boronate. The pK_a value concerned was determined to be 7.96, which is somewhat lower than that reported for phenylboronic acid ($pK_a = 8.7$),[25] probably as a result of the electron-withdrawing effect of the aminomethyl group. We conclude that L^1 is present in the tetragonal form over a wider pH range than L^2.

The ¹¹B NMR chemical shift of L^1 under basic conditions is −11.4 ppm, and that of L^2 is −16.6 ppm. This difference reflects the different electronic environments of the boron atoms in the two ligands and confirms the presence of a B–N interaction in L^1, and the absence of such an interaction in L^2.

Relaxometric characterization of the Gd³⁺ complexes: The Gd³⁺ complexes of L^1 and L^2 were synthesized from equimolar amounts of GdCl₃ and ligand in water at room temperature. The pH value was maintained at 5.5–6.5 during this synthesis.

The efficiency of an MRI CA is generally expressed in terms of relaxivity (r_{ip} in s⁻¹mM⁻¹), a parameter that indicates the ability of the CA to shorten the relaxation times of solvent water protons. Relaxivity is usually considered to be the result of a combination of inner-sphere (r_1^{is}) and outer-sphere contributions (r_1^{os}), which arise from the water molecules directly coordinated to the metal center and those freely diffusing around it, respectively.[1–4] Sometimes, an additional contribution originating from second-sphere water molecules can be identified. These water molecules are not directly coordinated to the metal ion but are bound to the complex through hydrogen bonds or other relatively weak interactions.

The inner-sphere contribution is described by Solomon–Bloembergen–Morgan theory [Equations (1)–(4)].[37]

$$r_1^{is} = \frac{[C] \cdot q}{1000 \cdot 55.56 \cdot (T_{1M} + \tau_M)} \quad (1)$$

$$(T_{1M})^{-1} \propto \frac{D_{is}}{r^6} J(\omega_I, \omega_s, \tau_{ci}) \quad (2)$$

$$(\tau_{ci})^{-1} = (\tau_M^{-1} + \tau_r^{-1} + \tau_{is}^{-1}) \quad (3)$$

$$(\tau_{is})^{-1} \propto K_i \Delta^2 J(\omega_s, \tau_v) \quad (4)$$

[C] is the concentration of the Gd³⁺ complex, q is the number of water molecules in the first coordination sphere of the metal ion, T_{1M} is their proton relaxation time, r is the Gd³⁺–H$_{water}$ distance, J is the spectral density function, τ_{ci} ($i = 1, 2$) are the overall correlation times for the dipolar nucleus–electron interaction, τ_M is the mean residence lifetime of the water molecules in the inner coordination sphere, τ_r is the reorientational correlation time of the GdH$_{water}$ vector, τ_{is} is the averaged relaxation time of the Gd³⁺ unpaired electrons, D_{is} and K_i are constants related to the nuclear and electron relaxation mechanisms, respectively, Δ^2 is the square of the transient zero field splitting (ZFS) energy, τ_v is the correlation time for the processes modulating the ZFS

Hamiltonian, and ω_s and ω_I are the electron and proton Larmor frequencies, respectively.

At pH 4.5 and 298 K, the relaxivities (measured at 20 MHz) of GdL¹ and GdL² are 5.7 and 4.7 s⁻¹mM⁻¹, respectively. These values are similar to those reported for Gd³⁺ complexes of other DTPA-bisamides.[38,39] The pH dependence of the relaxivities of the complexes increases significantly at low and high pH values (Figure 1). At pH < 2 both
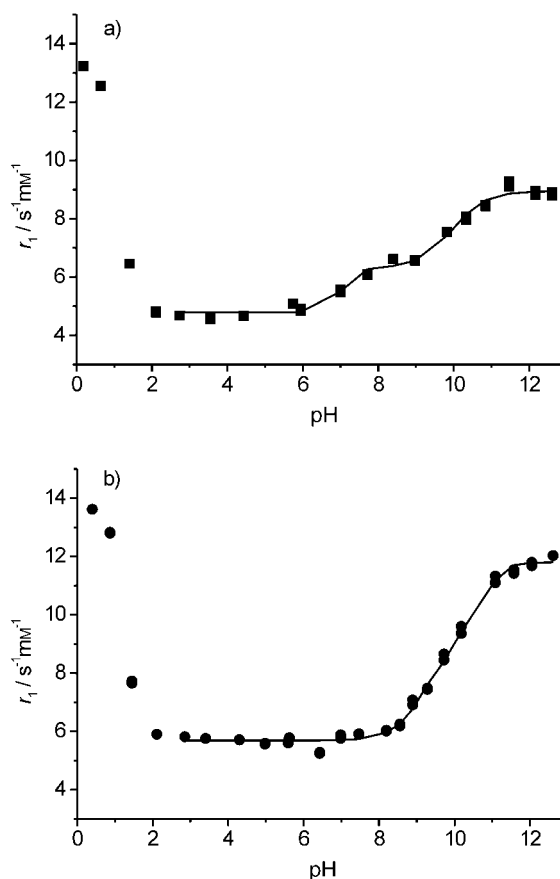

Figure 1. pH dependence of the relaxivity of a) GdL² and b) GdL¹ at 298 K and 20 MHz. The curves shown for pH > 2 are the result of fitting the data to Equations (5)–(7).

complexes show a steep increase in relaxivity to about 13 s⁻¹mM⁻¹, which is comparable to the relaxivity of the Gd³⁺ aquo ion. This behavior can be ascribed to decomplexation of the Gd³⁺ ion. At the other end of the profile, the relaxivity of GdL² begins to rise at pH 5–6 and the curve shows a jump in relaxivity centered around the pK_a of the boron functionality. In contrast, the relaxivity of GdL¹ only begins to rise when a pH value of 8–9 is reached. In both cases, the increase in relaxivity observed in the basic pH region (pH > 9) is most likely to be caused by activation of the prototropic exchange mechanism.[39]

DTPA-bisamides generally have relatively long exchange lifetimes, τ_M. The relaxivity of a complex of this size with a fast water exchange rate is usually governed mainly by changes in the rotational correlation time. However, when

the water exchange becomes sufficiently slow, τ_M starts to play a role as well. Any phenomenon that speeds up the exchange of the water protons between the complex and the bulk solvent results in an increase in the relaxivity.[1–4]

To evaluate the (whole) water exchange rates of GdL^1 and GdL^2, we determined the transverse ^{17}O relaxation rate for water in samples containing the complexes as a function of the temperature (Figure 2). An optimal fit of the experi-
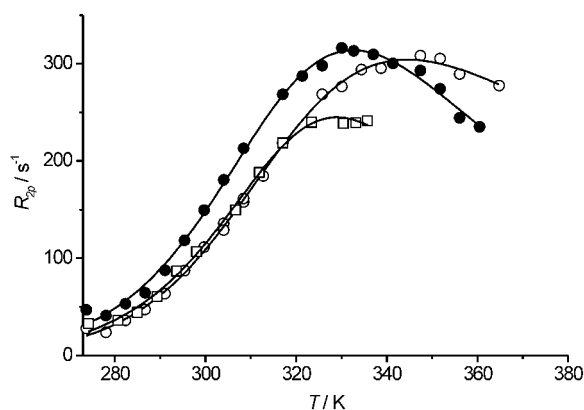

Figure 2. Temperature dependence of the ^{17}O transverse relaxation rate of a solution of GdL^1 (18.7 mM) at pH 6.0 (□), and of a solution of GdL^2 (25 mM) at pH 4.3 (●) and at pH 12.0 (○).

mental data with the Swift–Connick equations[40,41] was obtained for the τ_M values compiled in Table 1. The exchange lifetime of water in a solution of GdL^2 was found to be 25 %

Table 1. Water exchange lifetimes (τ_M) of GdL^1 and GdL^2, determined from water ^{17}O NMR relaxation rate ($1/T_2$) measurements. Standard deviations are given in parentheses.

Complex	pH	τ_M [μs]
GdL^1	6.0	3.0 (0.2)
GdL^2	4.3	4.1 (0.3)
GdL^2	12.0	2.9 (0.2)

greater at pH 4 than under basic conditions. This difference may be ascribed to the change in the overall charge of the complex from +2 at acidic pH values to −2 under basic conditions. A greater overall negative charge favors the dissociative process by which water molecules leave the complex and thus accelerates water exchange.[42] However, the observed change in the water exchange rate is not sufficient to account for the increased relaxivity observed at basic pH values (Figure 1). This was confirmed by a simulation of the longitudinal relaxation of a water molecule at 20 MHz produced from the τ_M value obtained from the ^{17}O NMR measurements (see Table 1), with all other parameters set to those of GdDTPA-bismethylamide (GdDTPA-BMA).

The pH profiles of the relaxivities of GdDTPA-bisamides generally show a sudden increase in relaxivity at basic pH as a result of the activation of prototropic exchange, which removes the quenching effect of the slow (whole) water exchange on the relaxivity. [39] Prototropic exchange can be

catalyzed both by H$^+$ and by OH$^-$ ions. It has been reported that the prototropic exchange rate is modulated by the overall charge of the complex under basic conditions; exchange is faster for positively charged and slower for negatively charged complexes.[39] This effect has been explained in terms of the ease of access of OH$^-$ ions to the coordinated water molecule. It is likely that the activation of prototropic exchange plays a role in the relaxivity enhancement observed for the two complexes GdL^1 and GdL^2 under basic conditions.

Comparison of the pH dependence of the relaxivities of GdL^1 and GdL^2 with the profiles of other GdDTPA-bisa-mide complexes reveals that the relaxivity of GdL^2 begins to increase at an unusually low pH value.[39,43] The presence of a jump in relaxivity around the pK_a value of the boronic functions of GdL^2 suggests that this phenomenon is related to the formation of the negatively charged boronate group. Inspection of molecular models reveals that this complex may easily adopt a conformation in which the boronate function is in close proximity to the Gd^{3+} ion. Therefore, a possible explanation for this jump in relaxivity is the presence of second-sphere water molecules near the negatively charged boronate group. These water molecules may be hydrogen bonded to the boronate function. The boronic groups in GdL^1 have a substantially higher pK_a value (>12) than those in GdL^2. The boronic acid moiety in GdL^1 has no overall charge in the pH range investigated and is much less effective at attracting second-sphere water molecules.

The pH profiles of the two complexes were fitted with Equation (6), which is derived from Equations (2) and (5). In these equations, k_{ex} is the exchange rate of the bulk water and k_{exb} is the rate of prototropic exchange catalyzed by hydroxy ions. Terms accounting for the contribution made by second-sphere and outer-sphere water molecules (r_1^{os}) are included. The concentration of free boronate functions, C_b is given by Equation (7), which can be derived from the equilibrium constant of the boric acid–boronate equilibrium and the appropriate mass balances.

$$\tau_M = (k_{ex} + k_{exb}[OH^-])^{-1} \tag{5}$$

$$r_{1p}^{obs} = \frac{C_{tot}q}{1000 \cdot 55.56 \cdot [T_{1M} + 1/(k_{ex} + k_{exb}[OH^-])]} + \frac{C_b w}{1000 \cdot 55.56 \cdot T_{1M}''} + r_1^{os} \tag{6}$$

$$C_b = \frac{K_b \cdot C_{tot}}{K_b + [H^+]^2} \tag{7}$$

C_{tot} is the molar concentration of the paramagnetic complex, C_b is the molar concentration of the complex in the boronate form, T_{1M} is the proton relaxation time of the coordinated water molecule, q is the number of inner-sphere water molecules, w is the number of second-sphere water molecules in the boronate form of the complex, and T_{1M}'' is their proton relaxation time. We assumed that the residence time of these water molecules is very short compared to T_1'' ($\tau_M'' \ll T_{1M}''$). We disregarded any contribution from exchange of the amide protons and the contribution of the amino

groups in the two ligands to the formation of a second-sphere hydration shell since these functional groups are relatively far from the paramagnetic center. An excellent fit was obtained for the pH profile of the relaxivity of GdL^1 when the number of second-sphere water molecules (w) was fixed at zero. For GdL^2, an optimal fit was obtained with $w/T''_{1M} = 8.48 \times 10^4\,\text{s}^{-1}$. The curves obtained are shown in Figure 1 and the best-fit values for the prototropic exchange rate constants of the two ligands are listed in Table 2, together with

Table 2. Prototropic exchange rates determined from the best-fit pH-dependence curves of the relaxivities of GdL^1 and GdL^2 at 20 MHz and 25 °C.[a] The exchange rates of Gd^{3+} complexes of other DTPA-bisamides are included for comparison.

Ligand	$k_{exb}\,[\text{s}^{-1}\,\text{M}^{-1}]$	Reference
L^1	1.41×10^{10}	this work
L^2	5.68×10^9	this work
7[b]	4.6×10^8	[39]
8[b]	8.6×10^{10}	[39]
9[b]	1.2×10^{10}	[39]

[a] See the main text for details. [b] The structures of ligands 7–9 are shown in Scheme 5.

literature values for other relevant Gd^{3+} complexes of DTPA-bisamides (Scheme 5).[39] The prototropic exchange rate constants obtained for GdL^1 and GdL^2 are in good agreement with the general trend of increasing prototropic exchange rate with increasing overall complex (positive) charge.
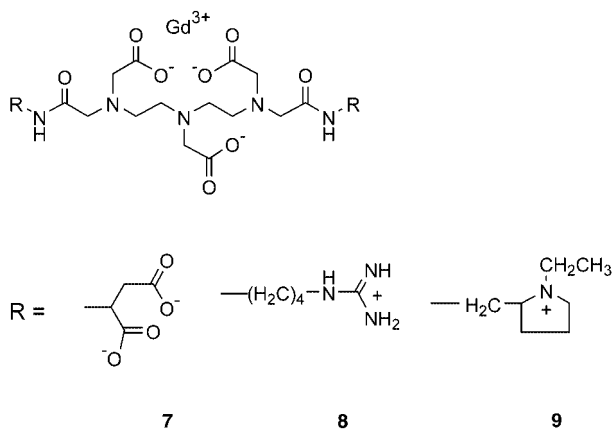
Scheme 5. Structures of the DTPA-bisamide ligands mentioned in Table 2.

We cannot exclude the possibility that the boronate function also catalyzes boronic prototropic exchange. However, inclusion of additional terms in Equation (6) to account for this catalytic effect did not lead to a better fit of the pH profile of the relaxivity.

The parameters that influence the relaxivity can be evaluated by measuring its field dependence (nuclear magnetic relaxation dispersion; NMRD) and fitting this experimental data to the values calculated by using the Solomon–Bloembergen–Morgan theory.[44–46] The large number of parameters involved in this model makes it advisable to determine as many of them as possible by independent techniques. These values can then be fixed during fitting of the NMRD profile. The NMRD profiles of GdL^1 and GdL^2 were recorded at 298 K and pH 6 and are shown in Figure 3. The
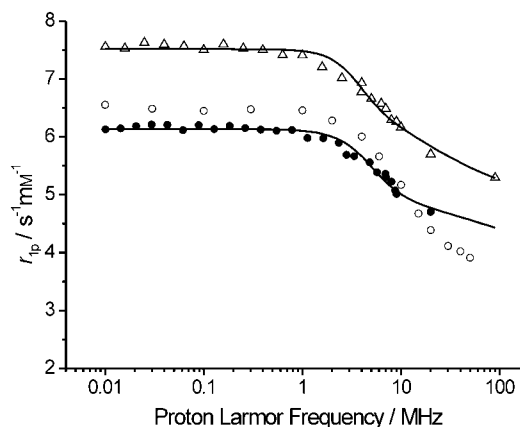
Figure 3. NMRD profiles of GdL^1 ($\triangle$), GdL^2 ($\bullet$), and GdDTPA-BMA ($\circ$), measured at 298 K.

NMRD profile of GdDTPA-BMA is included in this figure for comparison. At the pH value tested, the relaxivities of GdL^1 and GdL^2 are not significantly influenced by catalysis of the prototropic exchange or by the presence of second-sphere water molecules. We therefore assumed that the residence time of the water protons is determined by the "whole water" exchange rate, which was measured independently from the water ^{17}O transverse relaxation rates (see above). The experimental data were fitted to the theoretical values obtained from the Solomon–Bloembergen–Morgan theory. At low field, the relaxivities of Gd^{3+} complexes are mainly determined by the electronic relaxation time, τ_s. The relatively low relaxivities of GdL^1 and GdL^2 at low field compared to those of DOTA-like Gd^{3+} complexes under the same conditions ($r_1 \approx 12\,\text{s}^{-1}\,\text{mM}^{-1}$) are indicative of short electronic relaxation times, as observed for other acyclic ligands with low symmetry.[43] By using standard parameter values for a (distance of closest approach of a second-sphere water molecule, 3.8×10^{-10} m), D (relative diffusion coefficient of a complex and a water molecule, $2.24 \times 10^{-9}\,\text{m}^2\text{s}^{-1}$), and r (Gd–H distance for an inner-sphere water molecule, 3.1×10^{-10} m) and fixing the value of τ_M to that determined previously from the ^{17}O T_2 value, we calculated the electronic relaxation times at zero field (τ_{so}) and the τ_r values of the complexes. The results are compiled in Table 3. The relaxivities of GdL^1 and GdL^2 observed using the NMRD technique are higher than that observed for GdDTPA-BMA. This result can be ascribed to the higher rotational correlation times of GdL^1 and GdL^2 since this pa-

Table 3. Parameters obtained from the best fit of the NMRD profiles (25°C) of GdL^1 and GdL^2 to the Solomon–Bloembergen–Morgan model. GdDOTA[a] and GdDTPA data are included for comparison.[38]

	GdL^1	GdL^2	GdDTPA-BMA	GdDOTA
τ_v [ps]	35±2	23±2	25±1	11±1
Δ^2 [10^{19} s^{-2}]	2.3±0.1	4.5±0.1	4.1±0.2	1.6±0.1
τ_{so} [ps]	105±7	81±12	81±5	473±52
τ_r [ps]	214±11	186±22	66±11	77±4

[a] DOTA, tetraazacyclododecane.

rameter is the main factor governing the relaxivity under these conditions.

The τ_{so} values are relatively low and, as stated above, are typical for structures with low symmetry.[47] The reorientational correlation times (τ_r) of GdL^1 and GdL^2 are higher than those of GdDOTA and GdDTPA, which is in accordance with the higher molecular masses of GdL^1 and GdL^2.

Interaction of GdL^1 and GdL^2 with saccharides: The formation constants of the adducts of the two Gd^{3+} complexes (GdL^1 and GdL^2) with Neu5Ac were compared with those of the adducts formed with competing monosaccharides to evaluate the in vivo selectivity of the ligands for sialic acid. The interaction of Gd^{3+} complexes with macromolecular substrates is often evaluated by means of the well-established proton relaxation enhancement technique.[48,49] This approach exploits the increase in the observed water proton longitudinal relaxation rate that occurs as a result of the increase in the rotational correlation time upon formation of the adduct. Unfortunately, the large τ_M values of GdL^1 and GdL^2, combined with the small change in τ_r that occurs upon interaction with monosaccharides hampered determination of the formation constants by this method. We therefore exploited an approach developed by Springsteen and Wang,[26] which we adapted to suit our study.

The formation constants of the boronate esters of GdL^1 and GdL^2 and those of the saccharide adducts of these esters were measured by means of competitive titrations at pH 7.4. First, the formation constants of the esters formed by the complexes upon treatment with Alizarine Red S (ARS) were determined by measuring the change in fluorescence that occurred upon interaction. The association constants of the esters of GdL^1 and GdL^2 with the sugar under investigation were determined by titrating solutions of the complex with both ARS and the sugar in question and monitoring the change in fluorescence emission. In addition to Neu5Ac, methyl β-D-galactoside, methyl α-D-mannoside, and D(+)-glucose were studied for comparison. Methyl β-D-galactoside and methyl α-D-mannoside are models of units commonly present in glycan chains; glucose occurs at relatively high concentrations in the blood. The systems can be described by the equilibrium constants and mass balances defined in Equations (8)–(13).

$$K_1 = \frac{[BARS]}{[B][ARS]} \tag{8}$$

$$K_a = \frac{[BS]}{[B][S]} \tag{9}$$

$$C_{tARS} = [ARS] + [BARS] \tag{10}$$

$$C_{tS} = [S] + [BS] \tag{11}$$

$$C_{tB} = [B] + [BS] + [BARS] \tag{12}$$

$$I = \chi_{ARS} \cdot I_{ARS} + \chi_{BARS} \cdot I_{BARS} = I_{ARS} + \chi_{BARS} \cdot (I_{BARS} - I_{ARS}) \tag{13}$$

[S], [B], [ARS], [BARS], and [BS] are the molar concentrations of the saccharide, the free boron functionalities (both in the boronic and in the boronate form), free ARS, the boronate ester formed with ARS, and the boronate ester formed with the saccharide, respectively. C_{tARS}, C_{tS}, and C_{tB} are the total concentrations of ARS, the saccharide, and the boronic acid groups, respectively. The molar fractions of ARS and of its boronic acid ester are denoted as χ_{ARS} and χ_{BARS}, while I_{ARS} and I_{BARS} are their specific emissions. K_1 and K_a are the conditional association constants for association of the boron function concerned with ARS or the saccharide, respectively. The formation of intra- and intermolecular boronic esters with a boronic function/sugar ratio of 2:1 was neglected and the interactions of the two boronic functions present in each complex were regarded as independent. The concentration of the boronic acid was taken as double that of the Gd^{3+} complex for the calculation. By fitting the fluorescence data with Equations (8)–(13), we determined the formation constants of the adducts formed by GdL^1 and GdL^2 with ARS to be 1958±205 and 12433±2424 mol^{-1}L, respectively. Figure 4 shows the fluorescence data for the binding of GdL^1 and GdL^2 with ARS in competition with the various sugar derivatives. We carried out a least-squares fit of the data collected during the competition experiments to the described model by using the abovementioned formation constants for association with ARS. The results are listed in Table 4.

Both GdL^1 and GdL^2 interact considerably more strongly with sialic acid than with the other saccharides studied. Both complexes show good selectivity for sialic acid with respect to two of the most common saccharides present in glycan chains, methyl α-mannopyranoside and methyl β-galactopyranoside. Surprisingly, the formation constants of both complexes for association with sialic acid are also about two to three times greater than those of their glucose adducts. The α-furanose form of glucose is known to interact relatively strongly with phenylboronic acid and its derivatives since the cis-1,2-diol function in this anomeric form of the sugar is highly preorganized for the formation of boronate esters.[50–53] However, this anomeric form has an abundance of only 0.14% at anomeric equilibrium. The more abundant pyranose forms do not interact strongly with boronates and, consequently, the overall stability constant of the boronate ester is relatively low. These interactions may be even weaker in vivo than in vitro since the anomeric equilibrium of glucose is established very slowly and is rate determining for the formation of boronate esters of the furanose form. In vitro measurements taken after a short equilibra-
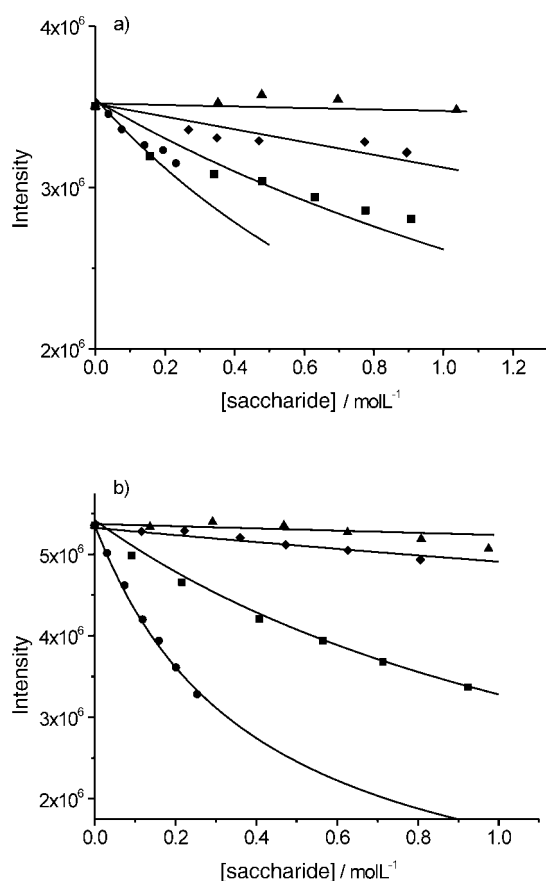
Figure 4. Intensity of the emission at 616 nm upon excitation at 468 nm of an aqueous solution of 1×10^{-5} M ARS, 1 mmol GdL^1 (a) or GdL^2 (b), 0.1 M sodium phosphate monobasic buffer (pH 7.4), and various amounts of N-acetylneuraminic acid (●), D-glucose (■), methyl α-D-mannoside (▲), or methyl β-D-galactoside (◆).

Table 4. Association constants (K_a) of some saccharides with GdL^1 and GdL^2 in 0.10 M phosphate buffer, pH 7.4. Each value shown is the average of duplicate measurements. Standard deviations are given in parentheses.

	K_a [mol^{-1} L][a]	
	GdL^1	GdL^2
N-acetylneuramic acid	3.30 (0.55)	50.43 (4.61)
D-glucose	1.70 (0.23)	15.19 (1.04)
Methyl α-D-mannoside	0.19 (0.08)	_[b]
Methyl β-D-galactoside	0.43 (0.10)	0.96 (0.48)

[a] The boronic functions present in each complex were regarded as independent (see the main text for details). [b] Not measured.

tion time can be expected to result in apparent formation constants for association with glucose even lower than those reported in Table 4. The relatively strong interaction of the two complexes with sialic acid as compared to that with glucose and the other two monosaccharides investigated is very promising for the development of sialic acid sensors.

The interaction of GdL^2 with sialic acid is considerably stronger than that of phenylboronic acid with this sugar ($K_a = 11.6$ M^{-1}). This observation reflects the synergetic effect of the charged protonated amine functions of GdL^2 on the binding of sialic acid. It is evident, however, that

GdL^1 interacts much less effectively than GdL^2 or phenylboronic acid with all the saccharides studied. Low preorganization of the sensing moiety and/or steric hindrance around the boronic group are possible causes of the weak interactions observed for this complex.

The two boronate units present in each of the complexes GdL^1 and GdL^2 may allow two-site binding of sialylated cell surfaces. As a result, the binding of these complexes might be considerably stronger than expected on the basis of the association constants reported in Table 4.

Studies on cell interactions: We used a radioactive nuclide and exploited the excellent sensitivity offered by radiometric methods to assess the capability of lanthanide complexes of L^1 and L^2 to discriminate between cells presenting different amounts of sialic acid on their surfaces. We investigated the interaction of ^{153}SmL^1 and ^{153}SmL^2 with C6 rat glioma cells, before and after treatment with neuraminidase. Like most higher animal cells, C6 rat glioma cells have been reported to have exposed sialic acid on their surfaces.[33]

In each experiment, one million cells were transferred to each of the six wells of a multiwell plate. The cells in three of the six wells were treated twice with neuraminidase according to a published procedure[32] to remove most of the sialic acid exposed on the cell surface. All cells were incubated with the complex under investigation (2.6 pmol ^{153}SmL^1 or ^{153}SmL^2) for 30 or 60 min at 37°C. Some experiments were carried out at 0°C to minimize the occurrence of internalization phenomena. After removal of the test solution, the cells were washed twice with phosphate-buffered saline and detached from the plate by treatment with 1 M NaOH. The radioactivity of the cell suspension in NaOH was measured to determine the amount of complex retained by the cells.

A modified version of the procedure described above was used to investigate whether internalization of the two complexes (^{153}SmL^1 and ^{153}SmL^2) occurs at 37°C. In these experiments, the cells were incubated with the complex and washed with phosphate-buffered saline, then treated with glycine buffer at pH 2.8. At this pH value, the boronic functional groups of both SmL^1 and SmL^2 are in their trigonal forms (see above), which do not interact with vicinal diol functions. Under these conditions, any SmL^1 or SmL^2 bound to sialic acid end groups at the cell surface is removed. The residual activity measured after detachment of the cells from the plate affords an estimate of the amount of internalized complex.

The results of these experiments are expressed as the difference between the residual activity of the cells not treated with neuraminidase and that of the cells that were treated (A, see Eq. (14)).

$$A = \frac{a_1 - a_2}{a_0} \times 100 \qquad (14)$$

The term a_0 represents the total radioactivity of the solution initially added to the cells, a_1 is the final radioactivity of cells not treated with neuraminidase, and a_2 is the final radioactivity of cells previously treated with neuraminidase.

Each experiment was repeated at least twice and the measured A values listed in Table 5 are the average percent residual activities measured.

Table 5. Residual activity expressed according to Eq. (14). The data are average values calculated from the results of at least two independent experiments in which each measurement was carried out in triplicate. Standard deviations are given in parentheses.

| | Temp [°C] | A [%] | |
		30 min	60 min
$^{153}SmL^1$	37	_[a]	1.80 (0.95)
$^{153}SmL^1$ (glycine treatment)	37	_[a]	1.70 (0.89)
$^{153}SmL^2$	0	2.02 (0.10)	7.62 (1.15)
$^{153}SmL^2$	37	3.27 (0.40)	6.20 (0.30)
$^{153}SmL^2$ (glycine treatment)	37	0.22 (0.15)	0.13 (0.08)

[a] Not determined.

The results for $^{153}SmL^2$ point to a dominant effect of the concentration of surface-bound sialic acid on the amount of complex that is retained by the cells. For $^{153}SmL^1$ the results are less clear and, if any binding occurs, the relationship between the extent of binding and the sialic acid concentration on the cell surface is much weaker than for $^{153}SmL^2$. No significant difference in residual activity was observed when experiments were carried out with $^{153}SmL^2$ at different temperatures. The surface binding of this complex seems to be unaffected by temperature.

The results of the experiments carried out with glycine treatment to investigate whether internalization processes occur indicate that $^{153}SmL^2$ is not internalized in any appreciable quantity. The residual activity for $^{153}SmL^1$ after treatment with glycine suggests that a slow internalization process exists. These results provide only a qualitative indication of the influence of sialic acid on the binding of the two complexes since the total quantity of sialic acid present on each cell surface was not determined. However, our observations concerning the surface binding of the two $^{153}Sm^{3+}$ complexes are in line with the relative values of the interaction constants measured for the two Gd^{3+} complexes and sialic acid (determined from the stability constants of the adducts concerned; see above).

By assuming that the residual activity (6.2%) of the cells treated with 2.6 pmol $^{153}SmL^2$ at 37 °C corresponds to the amount of this complex bound to sialic acid residues on the cell surface, we estimated that 1.10^5 complex molecules are bound by each cell.

Conclusions

We believe that recognition of sialic acid in living systems by MRI contrast agents is of importance for the detection of various malignancies. We designed and synthesized two new ligands for lanthanide ions, L^1 and L^2, and characterized their complexes. Gd^{3+} and $^{153}Sm^{3+}$ complexes of L^2 showed very promising properties that may be useful in the development of sialic acid sensors. GdL^2 has a fairly high interaction constant with Neu5Ac and is selective for the target over

other competing saccharides. The interaction of the corresponding ^{153}Sm complex with C6 rat glioma cells appears to be dependent on the concentration of sialic acid present on the cell surface. L^1 showed less favorable properties, although the selectivity of its Gd^{3+} complex for sialic acid with respect to competing saccharides is good. The reasons for the less promising performance of L^1 remain to be investigated further but the flexibility of the structure and steric hindrance around the boronic function could play an important role in reducing the affinity of its Ln^{3+} complexes for sugars.

The relaxometric properties of the two complexes are consistent with those of other Gd^{3+} complexes of DTPA-bisamides. Since the relaxometric parameters of this class of compounds are not optimal, a further improvement in the performance of these systems might be achieved by conjugating the recognition moieties to ligands whose Gd^{3+} complexes have a more favorable water exchange rate (20–30 ns). Such complexes include phosphonate analogues of DOTA and DTPA, as well as DOTA and DTPA structures with extended ethylene bridges. Further improvements in the sensitivity of the complexes could be achieved by conjugating the targeting vectors and a number of Gd^{3+} chelates to a high-molecular-weight carrier.

Experimental Section

Materials: *N*-acetylneuraminic acid was purchased from Rose Sci. Ltd and used without further purification. The cell culture medium, Dulbecco's F12 minimal essential medium (DMEM-F12), was purchased from Sigma and supplemented with 10% fetal bovine serum (FBS; Gibco), L-glutamine (Sigma), and penicillin/streptomycin (Sigma). Earle's balanced salt solution (EBSS) medium was purchased from Sigma, as was neuraminidase from *vibrio cholerae*. ^{153}Sm oxide was produced at the Instituto Tecnológico e Nuclear (ITN), Lisbon with a specific activity greater than 5 GBq mg^{-1}. A stock solution of $^{153}SmCl_3$ was prepared by dissolving $^{153}Sm_2O_3$ in 0.1 M HCl. All other reagent-grade chemicals were purchased from commercial sources and used without further purification.

Physical methods: The NMR spectra were recorded on a Varian INOVA-300 spectrometer operating at 300, 75.5, and 96.2 MHz for ^1H, ^{13}C, and ^{11}B, respectively, or on a Varian VXR-400S spectrometer operating at 400, 100.6, and 128.3 MHz for ^1H, ^{13}C, and ^{11}B, respectively. 5-mm sample tubes were used. For measurements in D_2O, *tert*-butyl alcohol was used as an internal standard, with the methyl signal calibrated at $\delta = 1.29$ (^1H) or 31.3 ppm (^{13}C). ^{11}B chemical shifts are reported with respect to 0.1 M boric acid in D_2O (taken as the external standard). The results can be converted to the $BF_3 \cdot Et_2O$ scale as follows: $\delta(H_3BO_3 \text{ scale}) = \delta(BF_3 \cdot Et_2O \text{ scale}) - 18.7$ ppm. Spectra were recorded at 25 °C unless stated otherwise.

The pH values of the samples were measured at ambient temperature by using a Corning 125 pH meter with a calibrated microcombination probe purchased from Aldrich. The pH values were adjusted by addition of dilute solutions of NaOH and HCl.

The longitudinal water proton relaxation rates were measured on a Stelar Spinmaster spectrometer (Mede) operating at 20 MHz. The standard inversion-recovery technique (16 experiments, two scans) was used. The temperature was controlled with a Stelar VTC-91 air-flow heater equipped with a copper thermocouple (uncertainty: ± 0.1 °C).

The proton $1/T_1$ NMRD profiles were recorded on a Stelar-Fast-Field-Cycling relaxometer over a continuous range of magnetic field strengths from 0.00024 to 0.28 T, which corresponds to a proton Larmor frequency range of 0.01–12 MHz. The relaxometer was under complete computer

control and took measurements with an absolute uncertainty in $1/T_1$ of ±1%.

Variable-temperature ^{17}O NMR measurements were recorded at 2.1 T with a Jeol EX-90 instrument equipped with a 5-mm probe. A D_2O external lock was used. Experimental settings: spectral width, 10000 Hz; 90° pulse, 7 μs; acquisition time, 10 ms; 1000 scans; no sample spinning. Aqueous solutions containing 2.6% ^{17}O isotope (Yeda) were used. The transverse relaxation rates were calculated from the signal widths at half the maximum signal height.

Fluorescence emission spectra were recorded with a Spex/Jobin-Yvon Fluorlog 3 fluorescence spectrometer (Instruments s.a.).

A well counter (DPC-Gamma C) with a 12 Compaq DeskPro compatible computer was used for activity counting in the interaction studies.

Molecular modeling was performed with the HyperChem software (version 7.5) and the MM+ force field was used.

Di-*tert*-butyl-nitrilo-2,2′,2″-triethanamine-*N*,*N*-dicarboxylate (1): Compound **1** was prepared by the procedure proposed by Hamdaoui et al.[34] ^1H NMR (300 MHz; CDCl$_3$): δ = 5.36 (brs, 2H; NH or NH$_2$), 3.19 (m, 4H; CH$_2$), 2.76 (t, 2H; CH$_2$), 2.57 (4H, t; CH$_2$), 2.53 (m, 2H; CH$_2$), 2.06 (brs, 2H; NH or NH$_2$), 1.47 ppm (s, 18H; CH$_3$); ^{13}C NMR (75.48 MHz; CDCl$_3$): δ = 160.61 (OCON), 83.42 (Me$_3$CO), 61.19 (CH$_2$N), 58.50 (CH$_2$N), 44.04 (CH$_2$N), 42.95 (CH$_2$N), 32.73 ppm ((CH$_3$)$_3$O).

Di-*tert*-butyl-*N*″-(4,5-dihydro-1*H*-imidazol-2-yl)-nitrilo-2,2′,2″-triethanamine-*N*,*N*-dicarboxylate (2): A solution containing **1** (8.167 g, 23.57 mmol) and methylthioimidazoline hydroiodide (5.812 g, 23.57 mmol) in EtOH (160 mL) was stirred at reflux (bath at 75°C) for 5 h. The solvent was removed under reduced pressure and the resulting red oil was used for the next step without further purification. ^1H NMR (300 MHz; CDCl$_3$): δ = 3.78 (s, 4H; CH$_2$ imidaz), 3.42 (m, 2H; CH$_2$), 3.16 (m, 4H; CH$_2$), 2.68 (t, 2H; CH$_2$), 2.58 (t, 4H; CH$_2$), 1.44 ppm (s, 18H; CH$_3$); ^{13}C NMR (75.48 MHz; CDCl$_3$): δ = 160.07 (O$_2$CN), 156.74 (CN$_3$), 79.78 (OCMe$_3$), 54.70 (CH$_2$), 53.58 (CH$_2$), 42.88 (CH$_2$), 41.93 (CH$_2$), 38.93 (CH$_2$ imidaz), 28.53 ppm (CH$_3$).

N-(4,5-Dihydro-1*H*-imidazol-2-yl)-nitrilo-2,2′,2″-triethanamine (3): Compound **2** was redissolved in EtOH (20 mL), then HCl (20 mL, 37%) was added dropwise. This solution was stirred at RT for 1.5 h. The solvent was removed under reduced pressure. MeOH (6×100 mL) was added and then evaporated from the solution. The yellow foam obtained was dissolved in a minimum amount of a methanol/water mixture and the product was isolated by cation exchange chromatography on a DOWEX 50-W×8–200 (H$^+$ form) column. An elution gradient from 20 to 50% HCl (37% aq) in methanol was used. The solvent was removed under reduced pressure and the residue was taken up in water, then lyophilized. The HCl salt of **3a** (6.629 g, 87%) was obtained as a white powder. ^1H NMR (400 MHz; D$_2$O): δ = 3.72 (s, 4H; CH$_2$ imidaz), 3.42 (t, 2H; CH$_2$), 3.08 (t, 4H; CH$_2$), 2.80 (t, 4H; CH$_2$), 2.74 ppm (t, 2H; CH$_2$); ^{13}C NMR (300 MHz; D$_2$O): δ = 161.54 (CN$_3$), 53.10 (CH$_2$), 51.71 (CH$_2$), 44.41 (CH$_2$), 40.72 (CH$_2$), 37.74 ppm (CH$_2$).

N-(4,5-Dihydro-1*H*-imidazol-2-yl)-*N*′-(2-dihydroxyboranylphenyl)-nitrilo-2,2′,2″-triethanamine (4): Intermediate **3** (4.07 g, 12.56 mmol) was dissolved in a minimum amount of methanol/triethylamine (3:1 v/v, ca. 70 mL). A solution of 2-formylphenylboronic acid (1.88 g, 12.56 mmol) in the same solvent (320 mL) was added dropwise over 30 min. The mixture was stirred at room temperature for 6 h. The solvent was removed under reduced pressure and the residue was redissolved in methanol (100 mL). NaBH$_4$ (2.38 g, 62.9 mmol) was added carefully. The reaction mixture was stirred overnight, then the solvent was removed under reduced pressure. The residue was taken up in water (ca. 15 mL) and filtered. The product was isolated by cation exchange chromatography on an Amberlite CG50 (NH$_4^+$ form) column with an elution gradient from 50 mM to 2 M NH$_4$OH in water. The fractions containing the desired product were collected and lyophilized to give the carbonate salt of **4** (1.450 g, 3.25 mmol, 26%) as a pale yellow fluffy solid. ^1H NMR (300 MHz; D$_2$O; pH < 2): δ = 7.71–7.76 (m, 1H; ArH), 7.38–7.51 (brs, 3H; ArH), 4.33 (s, 2H; ArCH$_2$), 3.56 (s, 4H; CH$_2$ imidaz), 3.32 (t, 2H; CH$_2$), 3.27 (t, 2H; CH$_2$), 3.01–3.20 (brs, 6H; CH$_2$), 2.92 ppm (t, 2H; CH$_2$); ^{13}C NMR (300 MHz; D$_2$O; pH 7): δ = 161.49 (CN$_3$), 139.26 (C$_{arom}$), 134.39 (C$_{arom}$), 131.36 (C$_{arom}$), 130.05 (C$_{arom}$), 129.47 (C$_{arom}$), 54.21 (CH$_2$), 52.96 (CH$_2$), 51.91 (CH$_2$), 51.07 (CH$_2$), 45.66 (CH$_2$), 44.28 (CH$_2$ imidaz), 41.37 (CH$_2$),

38.18 ppm (CH$_2$). One of the aromatic carbon nuclei was not observed, probably because of severe line broadening.

3,9-Bis{6-[(4,5-dihydroimidazol-2-yl)aminoethyl]-10-[2-(dihydroxyboranylphenyl)]-2-oxo-3,6,9-triazadecyl}-6-carboxymethyl-3,6,9-triazaundecanedioic acid (L^1): A solution containing **4** (0.654 g, 1.47 mmol), DTPA-bisanhydride (0.262 g, 0.73 mmol), and zeolite KA in absolute ethanol (16 mL) was stirred at room temperature for 6 h. The suspension was filtered and the solvent was removed under reduced pressure. The residue was taken up in water and lyophilized to give L^1 as a pale yellow solid (0.840 g, 95%). ^{11}B NMR (300 MHz; D$_2$O; pH 9.0): δ = −11.4 ppm; ^1H NMR (300 MHz; D$_2$O; pH 6.4): δ = 7.32–7.43 (m, 2H; ArH), 7.13–7.24 (m, 4H; ArH), 7.03–7.13 (m, 2H; ArH), 3.87 (s, 4H; ArCH$_2$), 3.47 (s, 8H; CH$_2$ imidaz), 2.44–3.39 ppm (brs, 42H; CH$_2$); ^{13}C NMR (300 MHz; D$_2$O; pH 6.4): δ = 180.37 (CO), 175.33 (CO), 171.94 (CO), 161.33 (CN$_3$), 145.80 (very broad; CB), 141.79 (C$_{arom}$), 131.69 (CH$_{arom}$), 129.68 (CH$_{arom}$), 129.04 (CH$_{arom}$), 125.62 (CH$_{arom}$), 60.97 (CH$_2$), 60.56 (CH$_2$), 56.08 (CH$_2$ central), 54.35 (CH$_2$), 54.17 (CH$_2$), 53.94 (CH$_2$), 53.72 (CH$_2$), 52.15 (CH$_2$), 51.35 (CH$_2$), 45.47 (CH$_2$), 44.13 (CH$_2$ imidaz), 41.63 (CH$_2$), 38.38 ppm (CH$_2$). ESI-MS (positive): m/z: 1056.7 [M+3]$^+$.

3,9-Bis(*tert*-butyl-2-oxo-3,6-diazahexyl-*N*-carboxylate)-6-carboxymethyl-3,6,9-triazaundecanedioic acid (5): Compound **5** was prepared by following the procedure described by Carvalho et al.[35] ^1H NMR (300 MHz; CDCl$_3$): δ = 3.75 (s, 4H; CH$_2$CO), 3.64 (s, 4H; CH$_2$CO), 3.62 (s, 2H; CH$_2$CO), 3.16–3.32 (m, 12H; CH$_2$N), 3.10 (t, 4H; CH$_2$N), 1.30 ppm (s, 18H; CH$_3$); ^{13}C NMR (300 MHz; CDCl$_3$): δ = 173.82 (CO), 173.73 (CO central), 170.58 (CO), 159.82 (O$_2$CN), 82.65 (CMe$_3$), 58.42 (CH$_2$CO), 58.19 (CH$_2$CO), 56.23 (CH$_2$CO central), 53.15 (CH$_2$N), 52.97 (CH$_2$N), 40.89 (2×CH$_2$N), 29.38 ppm (CH$_3$).

3,9-Bis(2-oxo-3,6-diazahexyl)-6-carboxymethyl-3,6,9-triazaundecanedioic acid (6): A solution of **5** (2.50 g, 3.69 mmol) in pure trifluoroacetic acid (10 mL) was stirred for 12 h. The solvent was removed under reduced pressure, followed by addition and then evaporation of CH$_2$Cl$_2$ (3× 10 mL) then ether (10 mL). The residue was taken up in water, filtered, and lyophilized to give **6** (2.94 g, 97%) as a white solid. ^1H NMR (300 MHz; D$_2$O; pH 1): δ = 4.14 (s, 4H; CH$_2$CO), 4.11 (s, 4H; CH$_2$CO), 3.80 (s, 2H; CH$_2$CO), 3.62 (t, 4H; CH$_2$N), 3.55 (t, 4H; CH$_2$N), 3.30 (t, 4H; CH$_2$N), 3.22 ppm (t, 4H; CH$_2$N); ^{13}C NMR (300 MHz; D$_2$O; pH 1): δ = 174.48 (CO), 171.94 (CO), 169.80 (CO), 57.95 (CH$_2$N), 57.43 (CH$_2$N), 55.58 (CH$_2$N central), 54.15 (CH$_2$N), 51.95 (CH$_2$N), 40.53 (CH$_2$N), 38.61 ppm (CH$_2$N).

3,9-Bis[3-(dihydroxoboranylphenyl)-2-oxo-3,6-diazaheptyl]-6-carboxymethyl-3,6,9-triazaundecanedioic acid (L^2): A solution of **6** (2.94 g, 3.59 mmol), 3-formylphenylboronic acid (1.38 g, 9.20 mmol), and triethylamine (8.0 mL) in methanol (15 mL) was stirred at room temperature for 2 h. NaBH$_4$ was added carefully (1.39 g, 36.7 mmol). The resulting solution was stirred at RT for 12 h. The solvent was removed under reduced pressure and the residue was taken up in water (ca. 10 mL). The resulting suspension was filtered and the desired product was recovered from the solution by cation exchange chromatography on a DOWEX 50-W×8–200 (H$^+$ form) column. The column was washed with water, then the product was eluted with an aqueous ammonia solution (8%). The solvent was removed under reduced pressure. The residue was taken up in water and lyophilized to give L^2 (2.391 g, 90%) as a white powder. ^{11}B NMR (400 MHz; D$_2$O; pH 11.3): δ = −16.6 ppm; ^1H NMR (300 MHz; D$_2$O; pH 11.3; T=80°C): δ = 7.50–7.60 (brs, 4H; ArH), 7.52 (brs, 2H; ArH), 7.18–7.25 (brs, 2H; ArH), 3.78 (s, 4H; ArCH$_2$), 3.41 (t, 4H; CH$_2$N), 3.29 (s, 4H; CH$_2$CO), 3.21 (s, 4H; CH$_2$CO), 3.15 (s, 2H; CH$_2$CO), 2.81 (t, 4H; CH$_2$N), 2.75 ppm (brs, 8H; CH$_2$N); ^{13}C NMR (300 MHz; D$_2$O; pH 11.3; T=80°C): δ = 179.7 (CO), 175.7 (CO), 175.5 (CO), 138.6 (C), 132.3 (C), 131.1 (C), 128.2 (C), 127.0 (C), 126.7 (C), 60.1 (CH$_2$), 59.5 (CH$_2$), 59.1 (CH$_2$), 53.5 (CH$_2$), 52.9 (CH$_2$), 47.8 (CH$_2$), 39.4 (CH$_2$), 30.7 ppm (CH$_2$). ESI-MS (positive): m/z: 748.62 [M+3]$^+$

Preparation of the Gd^{3+} complexes: Complexation was carried out by addition of stoichiometric amounts of GdCl$_3$ to aqueous solutions of the ligands under weakly acidic conditions (5.5 < pH < 6.5) at room temperature. The formation of the complex was monitored by measuring the solvent proton relaxation rate ($1/T_1$). The small excess of free Gd^{3+} ions, which yielded a noticeable increase in the observed relaxation rate, was removed by centrifugation of the solution after adjustment to basic pH.

Competitive fluorescence assay: A modified version of the procedure developed by Wang et al was used.[26] The association constants of GdL[1] and GdL[2] with Alizarine Red S (ARS) were first determined. Two solutions, A and B, were prepared. Solution A contained ARS (ca. 1×10^{-5} M) and sodium phosphate monobasic buffer (0.1 M) at pH 7.4. Solution B was prepared by dissolving GdL[1] or GdL[2] in a portion of solution A to obtain a complex concentration of about 1 mM. The concentrations of ARS and phosphate monobasic buffer remained the same. Solution B was titrated into solution A to produce solutions with a constant concentration of ARS and a range of concentrations of GdL[1] or GdL[2]. The intensity of the emission at 616 nm was recorded. The excitation wavelength was set at 468 nm.

The association constants for interaction of GdL[1] or GdL[2] with various carbohydrates were measured in a second set of experiments. A set of solutions C was prepared by dissolving various amounts of the appropriate saccharide in solution B (2.5 mL). At least seven different solutions C were prepared for each saccharide, with a range of concentrations from 0 to 0.5 M. Glucose solutions were allowed to stand at least 20 h to allow them to reach anomeric equilibrium; the solutions C of the other sugars were allowed to stand at least 1 h. A sialic acid solution was prepared by dissolving the necessary amount of sialic acid in a minimum volume of water and adjusting the pH to 7.4 by addition of 1 M NaOH. This solution was then lyophilized and the amount of salt present in the residue was determined by recording the ^{1}H NMR spectrum of a weighed sample in the presence of a *tert*-butanol standard. Least-square analysis of the data obtained for solutions C was performed with the program Scientist for Windows by Micromath, version 2.0.

Cell interaction studies: A sample of [153]SmCl₃ with a specific activity of 5 GBq mg⁻¹ was provided by the ITN in the form of a stock solution (1.9×10^{-3} M) in 1 N HCl.[54] [153]SmL (L=L[1] or L[2]) was prepared by adding [153]SmCl₃ (1 mCi) to a solution of the ligand in sodium acetate buffer (0.4 M, pH 5) to give a final ligand/[153]Sm mole ratio of 10:1. The radiochemical purity was determined by instant thin layer chromatography (GelmanSciences) with ammonium acetate as the mobile phase. The amount of bound metal averaged 98 % for all complexes.

C6 rat glioma cells were grown in 75-mL bottles in DMEM-F12 supplemented with 10 % FBS (Gibco), L-glutamine, and penicillin/streptomycin. The day before the experiments were carried out, the cells were counted and transferred to a six-well plate (10⁶ cells per hole). DMEM-F12 (4 mL) was added to each well and the cells were incubated overnight at 37 °C under 5 % CO₂.

Half the cells (three wells of each plate) were treated twice with neuraminidase according to the procedure described by Meyer et al.[55] The medium was removed and the cells were washed twice with EBSS medium (1.5 mL). Fresh EBSS medium (1.2 mL) was then added and the cells were allowed to adjust to the medium for 1 h at 37 °C. SmL[1] or SmL[2] (2.6 pmol, 3.333 KBq) was added to each well and the cells were incubated for up to 1 h at 37 or 0 °C. After appropriate time periods (30 and 60 min), the experiment was stopped by removing the medium and washing the cells twice with ice-cold phosphate-buffered saline (150 μL). The cells were then treated with glycine buffer (150 μL, 0.05 M glycine solution, pH adjusted to 2.8 with 1 N HCl) to distinguish between cell-surface-bound (acid-releasable) and internalized (acid-resistant) radioligand. We skipped this step (acid wash) in some of the experiments for comparative purposes. Finally, the cells were treated with 1 N NaOH (150 μL) and incubated at 37 °C for 10 min to detach them from the plates. The radioactivity was measured with a γ-counter. Each experiment was carried out simultaneously in triplicate and was repeated at least twice.

Acknowledgement

[1] A. E. Merbach, É. Tóth, *The Chemistry of Contrast Agents in Medical Magnetic Resonance Imaging*, Wiley, Chichester, **2001**.
[2] P. Caravan, J. J. Ellison, T. J. McMurry, R. B. Lauffer, *Chem. Rev.* **1999**, *99*, 2293.
[3] S. Aime, M. Fasano, E. Terreno, *Chem. Soc. Rev.* **1998**, *27*, 19.
[4] J. A. Peters, J. Huskens, D. J. Raber, *Prog. Nucl. Magn. Reson. Spectrosc.* **1996**, *28*, 283.
[5] V. Jacques, J. F. Desreux, *Top. Curr. Chem.* **2002**, *221*, 123.
[6] É. Tóth, L. Helm, A. E. Merbach, *Top. Curr. Chem.* **2002**, *221*, 61.
[7] M. Rudin, R. Weissleder, *Nat. Rev. Drug Discovery* **2003**, *2*, 123.
[8] R. J. Gillies, *J. Cell. Biochem.* **2002**, *Suppl. 39*, 231.
[9] S. A. Wickline, G. M. Lanza, *J. Cell. Biochem.* **2002**, *Suppl. 39*, 90.
[10] K. J. Potter, *J. Cell. Biochem.* **2002**, *Suppl. 39*, 147.
[11] A. D. Nunn, K. E. Linder, M. F. Tweedle, *J. Nucl. Med.* **1997**, *41*, 155.
[12] R. Schauer in *Carbohydrates in Chemistry and Biology, Vol. 3* (Eds.: B. Ernst, G. W. Hart, P. Sinay), Wiley-VCH, Weinheim, **2000**, p 227.
[13] R. Schauer, J. P. Kamerling, *New Compre. Biochem.* **1997**, *29b*, 243.
[14] R. Schauer, *Glycoconjugate J.* **2001**, *17*, 485.
[15] S. Kelm, R. Schauer, *Int. Rev. Cytol.* **1997**, *175*, 137.
[16] C. Traving, R. Schauer, *Cell. Mol. Life Sci.* **1998**, *54*, 1330.
[17] F. N. Lamari, N. K. Karamanos, *J. Chromatogr. B, Anal. Technol. Biomed. Life Sci.* **2002**, *781*, 3.
[18] G. A. Lemieux, K. J. Yarema, C. L. Jacobs, C. R. Bertozzi, *J. Am. Chem. Soc.* **1999**, *121*, 4278.
[19] A. P. Davis, R. S. Wareham, *Angew. Chem.* **1999**, *111*, 3160; *Angew. Chem. Int. Ed.* **1999**, *38*, 2979.
[20] S. R. Haseley, *Anal. Chim. Acta* **2002**, *457*, 39.
[21] T. D. James, S. Shinkai, *Top. Curr. Chem.* **2002**, *218*, 159.
[22] J. Böeseken, A. van Rossem, *Recl. Trav. Chim. Pays-Bas* **1912**, *30*, 392.
[23] J. Böeseken, *Chem. Ber.* **1914**, *46*, 2612.
[24] H. G. Kuivila, A. H. Keough, E. J. Soboczenski, *J. Org. Chem.* **1954**, *19*, 780.
[25] J. O. Edwards, R. J. Sederstrom, *J. Phys. Chem.* **1961**, *65*, 862.
[26] G. Springsteen, B. Wang, *Tetrahedron* **2002**, *58*, 5291.
[27] G. Wulff, *Pure Appl. Chem.* **1982**, *54*, 2093.
[28] T. Burgemeister, R. Grobe-Einsler, R. Grotstollen, A. Mannschreck, G. Wulff, *Chem. Ber.* **1981**, *114*, 3403.
[29] S. L. Wiskur, J. J. Lavigne, H. Ait-Haddou, V. Lynch, Y. H. Chiu, J. W. Canary, E. V. Anslyn, *Org. Lett.* **2001**, *3*, 1311.
[30] K. Djanashvili, L. Frullano, J. A. Peters, unpublished results.
[31] C. L. Hannon, E. V. Anslyn, *Bioorg. Chem. Front.* **1993**, 193.
[32] E. E. Simanek, G. J. McGarvey, J. A. Jablonowski, C.-H. Wong, *Chem. Rev.* **1998**, *98*, 833.
[33] O. L. Berezovskaya, V. Mares, G. G. Skibo, *J. Neurosci. Res.* **1995**, *42*, 192.
[34] B. Hamdaoui, G. Dewynter, F. Capony, J.-L. Montero, C. Toiron, M. Hnach, H. Rochefort, *Bull. Soc. Chim. Fr.* **1994**, *131*, 854.
[35] J. F. Carvalho, S. P. Crofts, S. M. Rocklage (Salutar Inc.), WO9110645, **1991**.
[36] R. M. Smith, A. E. Martell, *Critical Stability Constants, Vol. 2*, Plenum, New York, **1975**, p. 7.
[37] I. Bertini, C. Luchinat, *Coord. Chem. Rev.* **1996**, *150*, 1.
[38] D. H. Powell, O. M. Ni Dhubhghaill, D. Pubanz, L. Helm, Y. S. Lebedev, W. Schlaepfer, A. E. Merbach, *J. Am. Chem. Soc.* **1996**, *118*, 9333.
[39] S. Aime, E. Gianolio, A. Barge, D. Kostakis, I. C. Plakatouras, N. Hadjiliadis, *Eur. J. Inorg. Chem.* **2003**, 2045.
[40] T. J. Swift, R. E. Connick, *J. Chem. Phys.* **1964**, *41*, 2553.
[41] T. J. Swift, R. E. Connick, *J. Chem. Phys.* **1962**, *37*, 307.
[42] J. P. André, H. R. Maecke, É. Tóth, A. E. Merbach, *J. Biol. Inorg. Chem.* **1999**, *4*, 341.
[43] S. Aime, M. Botta, M. Fasano, E. Terreno, *Acc. Chem. Res.* **1999**, *32*, 941.

[44] I. Solomon, *Phys. Rev.* **1955**, *99*, 559.

[45] N. Bloembergen, *J. Chem. Phys.* **1957**, *27*, 572.

[46] N. Bloembergen, L. O. Morgan, *J. Chem. Phys.* **1961**, *34*, 842.

[47] R. B. Clarkson, A. I. Smirnov, T. I. Smirnova, R. L. Belford in *The Chemistry of Contrast Agents in Medical Magnetic Resonance Imaging* (Eds.: A. E. Merbach, É. Tóth), Wiley, Chichester, **2001**, p. 383.

[48] R. A. Dwek, *Monographs on Physical Biochemistry: Nuclear Magnetic Resonance (N.M.R) in Biochemistry. Applications to Enzyme Systems, Vol. 3*, Oxford University Press, New York, **1973**, p. 396.

[49] B. G. Jenkins, E. Armstrong, R. B. Lauffer, *Magn. Reson. Med.* **1991**, *17*, 164.

[50] G. de Wit, PhD Thesis, Delft University of Technology, **1979**.

[51] R. van den Berg, J. A. Peters, H. van Bekkum, *Carbohydr. Res.* **1994**, *253*, 1.

[52] J. C. Norrild, I. Søtofte, *J. Chem. Soc. Perkin Trans. 2* **2002**, 303.

[53] J. C. Norrild, H. Eggert, *J. Am. Chem. Soc.* **1995**, *117*, 1479.

[54] F. C. Alves, P. Donato, A. D. Sherry, A. Zaheer, S. Zhang, A. J. Lubag, M. E. Merritt, R. E. Lenkinski, J. V. Frangioni, M. Neves, M. I. M. Prata, A. C. Santos, J. J. P. Lima, C. F. G. C. Geraldes, *Invest. Radiol.* **2003**, *38*, 750.

[55] D. C. Mayer, O. Kaneko, D. E. Hudson-Taylor, M. E. Reid, L. H. Miller, *Proc. Natl. Acad. Sci. USA* **2001**, *98*, 5222.